Comparisons of Pressure and Temperature Activation Parameters for Amide Hydrogen Exchange in T4 Lysozyme†

Michelle E. Dixon,‡ T. Kevin Hitchens,§ and Robert G. Bryant*,‡

Department of Chemistry, University of Virginia, Charlottesville, Virginia 22901, and Department of Biological Sciences, Carnegie Mellon University, Pittsburgh, Pennsylvania 15213-2617

Received July 26, 1999; Revised Manuscript Received October 26, 1999

ABSTRACT: Activation enthalpies and entropies are reported for proton−deuteron exchange at 42 amide sites in T4 lysozyme and compared with activation volumes for the same residues obtained earlier [Hitchens, T. K., and Bryant, R. G. (1998) *Biochemistry 37,* 5878−5887]. There is no correlation found between activation volume and activation entropy or activation enthalpy. The activation enthalpy is linearly related to the activation entropy in part as a consequence of a relatively narrow sampling window for the rate constants that corresponds to a narrow range of activation free energy. A consequence of the entropy−enthalpy compensation is preservation of rank order of proton exchange. Variations in $\Delta H^{\ddagger}$, $\Delta S^{\ddagger}$, and $\Delta V^{\ddagger}$ for residues that are structurally close together in the folded protein suggest that there may be a variety of energetically distinct pathways for the access of solvent to these structurally related exchange sites.

Protein dynamics are critical to understanding protein function because the static structures resulting from X-ray crystallography do not, by themselves, account for the catalytic function of proteins. Evidence of protein structural fluctuations is available from many techniques including thermal factors from X-ray crystallography (*1, 2*), fluorescence quenching (*3*) and relaxation studies (*4*), nuclear magnetic resonance relaxation studies (*5*), and hydrogen exchange experiments (*6*−*10*). Considerable uncertainty remains about the details of the connection between structural fluctuations and function.

Amide proton−deuterium exchange in combination with nuclear magnetic resonance (NMR)[1] provides a high-resolution approach to measuring the integrated effects of protein structural fluctuations. Two-dimensional NMR spectroscopy provides the opportunity to measure isotope exchange rates at each amide site in a protein. The remarkable feature of amide hydrogen exchange is that the rate constants span approximately 8 orders of magnitude in a folded protein but are nearly degenerate in an unfolded or denatured protein. Several models have been proposed to understand this broad distribution of slow rates including global unfolding and solvent penetration mechanisms (*6*−*10*). All pathways involve structural fluctuations, and the limiting models, which are convenient for discussion, may not be uniformly applicable (*11, 12*).

Recently, we have characterized the pressure dependence of amide proton exchange rate constants for T4 lysozyme (*13*). Interpreted in the context of transition-state theory, these measurements provide activation volumes for the exchange processes at individual sites in the folded protein. The experimental conditions were chosen such that the protein was far from the denaturation transition. The $\Delta V^{\ddagger}$ values, while small, were found to vary substantially, and they did not correlate simply with secondary structural elements of the protein.

Here we extend the characterization of amide exchange kinetics in T4 lysozyme using conditions closely matching those of the pressure dependence study. The temperature dependence of the rate constants was measured, and the activation enthalpies and entropies were deduced using transition-state theory. We find that there is no significant correlation between the activation volumes and the activation enthalpies or activation entropies for the 42 residues studied. There is a remarkable linear correlation between the activation enthalpy and activation entropy, which may be understood in the context of the kinetic sampling window of the experiment. A direct consequence of this correlation is the preservation of the rank order of the hydrogen exchange throughout the temperature range studied.

MATERIALS AND METHODS

T4 Lysozyme and Sample Preparation. ^{15}N-Labeled T4 lysozyme as a thiol-free mutant (C54T/C97A) with properties similar to the wild-type lysozyme was prepared as described previously (*14*−*16*). Aliquots (1.2 mL) of labeled protein at 2.0 mg/mL in 50 mM Tris buffer/H_2O containing 0.02% sodium azide were lyophilized. These samples yielded a buffered 0.6 mM protein solution upon addition of 1.2 mL

† This work was supported by the National Institutes of Health (GM 34541) and the University of Virginia.

* Please send correspondence to: Robert G. Bryant, University of Virginia. Tel: (804) 924-1494. E-mail: rgb4g@virginia.edu.

‡ University of Virginia.

§ Carnegie Mellon University.

[1] Abbreviations: $\Delta H^{\ddagger}$, activation enthalpy; $\Delta S^{\ddagger}$, activation entropy; $\Delta V^{\ddagger}$, activation volume; $\Delta G^{\ddagger}$, activation free energy; NMR, nuclear magnetic resonance; Tris, tris(hydroxymethyl)aminomethane; D_2O, deuterim oxide; MHz, megahertz; HSQC, heteronuclear single-quantum coherence; *P*, pressure; WT*, C54T/C97A mutant of T4 lysozyme; pH*, uncorrected pH reading of D_2O solution.

10.1021/bi991718y CCC: $19.00
Published on Web 12/09/1999

of D_2O (99.9% D; Cambridge Isotope Laboratories, Andover, MA) at the beginning of each kinetic series.

Amide Hydrogen Exchange Experiments. For each sample, a set increment of 7 min was allowed to elapse between the rehydration of the sample and the commencement of the measured hydrogen exchange period ($t = 0$). First, a fixed time of 5 min was employed to dissolve the sample and adjust its pH*. The sample was dissolved in 1.2 mL of D_2O and the pH* was adjusted to a meter reading of 7.5 using a Sensorex mini pH electrode and an Orion pH meter (model 720A). The pH* readings were not corrected for deuterium isotope effects. The remaining 2 min were utilized as a temperature equilibration time for the sample, during which the samples were placed in a circulating, temperature-regulated water/ethylene glycol bath (VWR, model 1147) to facilitate rapid temperature equilibration.

Equilibrated samples remained in the circulating water/ethylene glycol bath to permit amide hydrogen exchange for variable but specific time periods. The temperature range studied was from 7 to 32 °C, with exchange times ranging from 0 to 220 min using 39 samples. At the end of the exchange period, the sample was removed from the circulating water bath and the sample pH* was titrated to 3.2, the amide exchange rate minimum. At this pH*, exchange is sufficiently slow to allow NMR data acquisition without a significant change in the amide hydrogen populations over the 80-min acquisition time. Using this hydrogen exchange quench method minimizes difficulties of temperature control because during the exchange period, the sample is in good thermal contact with a high-heat-capacity circulating water bath. Because the NMR acquisition times are long, the quench technique also permits accurate definition of the kinetic time points and permits sampling at times much shorter than the NMR data acquisition time. Further, the NMR assignments are independent of the conditions attained during the hydrogen exchange period. Samples were concentrated to 300 μL at 10 °C to obtain a sufficiently high concentration of protein for spectroscopic purposes and stored at 10 °C until data could be collected.

NMR Measurements. NMR data were all acquired at 500 MHz using a Varian Unity Plus 500 spectrometer. Two-dimensional (2D) spectra were processed using PROSA v. 2.8 (Güntert, P., and Dötsch, V., ETH, Zürich, Switzerland) and XEASY (Xia, T.-H., and Bartels, C., ETH, Zürich, Switzerland) NMR software. One-dimensional (1D) spectra were processed using Felix 97.0 NMR software (Molecular Simulations, Inc., San Diego, CA). Peaks in the sensitivity-enhanced 2D $^1H-^{15}N$ HSQC (*17*) spectra were assigned as described previously (*13*). Individual amide hydrogen peak intensities were measured in each $^1H-^{15}N$ HSQC spectrum after every exchange time so that a kinetic profile for each amide site at six temperatures was collected. Peak intensities within each 2D spectrum were normalized to the H^γ resonance of Val94 (−0.78 ppm) in the corresponding 1D ^1H spectrum acquired for all the samples to account for small differences in concentration or spectrometer characteristics among the samples.

The HSQC spectra were acquired at 25 °C with a spectral width of 6500 Hz in the directly detected dimension (^1H). Each acquisition consisted of 16 transients, each containing 1024 complex points, corresponding to a total acquisition time of approximately 80 min. The spectral width of the indirect dimension (^{15}N) was 1630 Hz and employed 128 complex points. Spectra were zero-filled to 2048 points in the directly detected dimension and to 512 points in the indirectly detected dimension, then processed according to the method of Kay and co-workers (*18*). 1D ^1H spectra were acquired and processed as previously described (*13*).

Data Analysis. The activation parameters for exchange at each amide site were determined by fitting the normalized peak intensities from 39 spectra acquired at six temperatures using the nonlinear least-squares fitting program NONLIN (*19, 20*). We adopt the formalism of transition-state theory to fit the cross-peak intensities directly, using eq 1:

$$I(T,t) = I_o e^{-[(k_b T/h)e^{-\Delta H(obs,\ddagger)/RT} e^{\Delta S(obs,\ddagger)/R}]t} \quad (1)$$

$I(T,t)$ is the normalized cross-peak intensity. The independent variables were temperature (T) and time (t). The fitted parameters were the initial cross-peak intensity (I_o) at time = 0, the activation enthalpy ($\Delta H^\ddagger_{obs}$), and the activation entropy ($\Delta S^\ddagger_{obs}$), and the constants are the Boltzmann constant (k_b), Planck's constant (h), and the gas constant (R).

The observed activation enthalpies ($\Delta H^\ddagger_{obs}$) may be written as the sum of four contributions (*13*):

$$\Delta H^\ddagger_{obs} = \Delta H_{K_{eq}} + \Delta H^\ddagger_{k_{OH}} + \Delta H_{K_W} - \Delta H_{Tris} \quad (2)$$

where $\Delta H_{K_{eq}}$ is the enthalpy change associated with the equilibrium between the solvent-accessible and solvent-inaccessible states of each amide site, $\Delta H^\ddagger_{k_{OH}}$ is the activation enthalpy of the base-catalyzed chemical exchange process, and ΔH_{K_W} and ΔH_{Tris} are the enthalpy changes associated with the dissociation of water and Tris buffer, respectively. Values for ΔH_{K_W} of +13.5 kcal mol^{-1} and ΔH_{Tris} of +11.3 kcal mol^{-1} have been reported (*21*). $\Delta H^\ddagger_{EX}$ denotes the sum of $\Delta H_{K_{eq}}$ and $\Delta H^\ddagger_{k_{OH}}$, which is equivalent to $\Delta H^\ddagger_{obs}$ − 2.2 kcal mol^{-1} based on substitution and rearrangement of eq 2. A similar treatment was applied to calculate $\Delta S^\ddagger_{EX}$ using values of −19.2 cal mol^{-1} K^{-1} for ΔS_{K_W} and +1.1 cal mol^{-1} K^{-1} for ΔS_{Tris} (*22*). Thus, $\Delta S^\ddagger_{EX}$ is $\Delta S^\ddagger_{obs}$ + 20.3 cal mol^{-1} K^{-1}.

Protection factors were calculated at 22 °C by determining the ratio of the predicted random coil exchange rate constant (k_{rc}) to the measured exchange rate constant (k_{obs}) at each amide site, using the method of Bai and co-workers (*23*):

$$P_f = \frac{k_{rc}}{k_{obs}} \quad (3)$$

The predicted random coil exchange rate constant is calculated for each site and is dependent on pH and the two residues flanking the amide site. Experimental rate constants were determined using NONLIN to fit the data to eq 4, where I is the normalized intensity of the HSQC cross-peaks. The independent variable was time (t). The fitted parameters were the initial intensity (I_o) and the rate constant (k_{obs}):

$$I(t) = I_o e^{-k_{obs}t} \quad (4)$$

Protection factors for wild-type T4 lysozyme were reported

Table 1: Measured Activation Enthalpies for WT* T4 Lysozyme in the Temperature Range 280−305 K

residue	$\Delta H^{\ddagger}_{EX}$ [a,b]		$\Delta S^{\ddagger}_{EX}$ [a,c]		P_f [d]	WT* P_f [e]	$\Delta V^{\ddagger}_s$ [f]
Phe4	18.0	(16.3, 19.8)	16.9	(11.2, 22.9)	3.3	4.3	−0.3
Lys16	23.5	(22.2, 24.8)	33.6	(29.4, 38.0)	3.8	6.0	−3.0
Ile17	13.6	(12.3, 14.9)	1.9	(−2.5, 34.2)	3.0	5.4	−3.7
Tyr18	19.0	(16.9, 21.2)	20.6	(13.3, 27.9)	3.2	4.7	3.6
Thr26	30.5	(28.4, 32.6)	56.3	(49.2, 63.4)	4.2	6.8	−2.7
Ile27	30.9	(28.6, 33.3)	55.5	(48.0, 63.5)	4.3	6.8	−12.9
Gly28	26.8	(24.5, 29.2)	44.3	(36.6, 52.6)	4.2	6.3	−0.7
Ile29	11.2	(9.3, 13.2)	−7.2	(−13.7, −0.5)	3.3	5.0	−4.4
His31	21.8	(17.3, 26.4)	31.1	(15.3, 46.8)	4.4	6.1	12.8
Leu33	24.2	(22.2, 26.1)	37.0	(30.3, 43.7)	3.0	6.0	6.6
Lys43	10.8	(6.1, 15.4)	−6.8	(−22.9, 9.2)	3.7	4.8	6.6
Glu45	17.9	(14.8, 21.0)	18.3	(7.6, 29.0)	3.2	5.2	−2.3
Leu46	23.3	(22.2, 24.5)	32.5	(28.7, 36.5)	3.4	6.0	−4.0
Asp47	29.4	(26.6, 32.2)	51.6	(42.2, 61.0)	4.0	6.4	−9.3
Lys48	18.1	(15.4, 20.8)	19.0	(9.6, 28.4)	3.3	5.4	−5.6
Ala49	15.7	(14.3, 17.0)	8.4	(3.9, 13.0)	3.9	5.4	−9.8
Ile50	26.2	(23.9, 28.6)	40.6	(32.7, 48.4)	3.8	6.3	−11.3
Ile58	25.7	(21.4, 29.9)	36.9	(22.6, 51.1)	4.1	6.9	−15.0
Thr59	34.0	(31.1, 37.0)	66.6	(57.1, 76.8)	4.3	6.8	−10.0
Glu62	10.4	(8.9, 12.1)	−8.6	(−14.0, −3.1)	2.9	4.3	−8.3
Glu64	17.3	(15.8, 18.8)	10.7	(5.6, 15.9)	4.0	5.1	0.4
Lys65	16.4	(15.3, 17.5)	10.5	(6.8, 14.2)	3.7	4.2	−4.9
Asp70	20.8	(17.4, 24.1)	20.2	(8.8, 31.4)	4.9	6.3	−7.8
Asp72	15.0	(13.0, 16.9)	1.7	(−4.8, 8.1)	4.2	5.6	0.9
Ala73	11.1	(10.1, 12.1)	−9.2	(−12.6, −5.8)	3.7	5.2	0.8
Gly77	17.2	(16.0, 18.4)	10.8	(6.8, 14.9)	4.9	6.2	1.4
Ile78	17.4	(14.4, 20.3)	9.8	(−0.1, 19.7)	4.1	6.3	1.5
Arg80	13.8	(12.7, 14.8)	0.7	(−2.8, 4.2)	3.9	5.0	0.8
Asn81	16.1	(15.2, 17.1)	9.9	(6.7, 13.0)	4.6	5.3	−4.1
Leu84	16.3	(15.2, 17.5)	9.3	(5.6, 13.2)	3.6	5.3	−6.3
Asp89	12.4	(11.3, 13.4)	−3.4	(−6.9, 0.2)	3.6	5.0	−0.3
Leu91	12.1	(9.2, 15.0)	−8.5	(−18.3, 1.2)	4.6	6.2	−4.6
Met106	18.4	(16.5, 20.3)	13.9	(7.6, 20.2)	4.8	5.5	−0.5
Gln123	15.9	(13.1, 19.2)	10.8	(1.0, 22.1)	3.7	4.7	−15.1
Trp126	19.7	(18.2, 21.3)	23.3	(18.1, 28.8)	3.3	4.5	−2.7
Ala129	20.7	(19.0, 22.4)	22.6	(16.9, 28.4)	4.2	5.5	−4.6
Ala146	16.6	(15.4, 17.8)	10.1	(6.1, 14.3)	4.2	5.1	−3.2
Lys147	18.3	(17.3, 19.4)	16.4	(12.8, 20.1)	3.9	4.5	2.6
Thr151	14.6	(13.3, 15.8)	4.2	(0.1, 8.5)	3.5	5.2	3.5
Thr155	7.3	(5.2, 9.5)	−18.4	(−25.6, −11.0)	3.7	5.0	1.2
Thr157	10.8	(9.5, 12.1)	−10.1	(−14.4, −5.6)	4.2	5.7	−9.2
Tyr161	14.2	(11.0, 17.5)	−1.4	(−12.3, 9.7)	4.6	5.6	−8.7

[a] 67% Confidence interval in parentheses. [b] In kcal mol^{-1}. [c] In cal mol^{-1} K^{-1}. [d] Calculated using the method of Bai and co-workers using the fitted rate constants at 22 °C (*23*). [e] Protection factors for the wild-type protein averaged over several pH values (*24*). [f] Volumes of solvent accessibility in cm^3 mol^{-1} (*13*).

by the Dahlquist group (*24*). Activation volumes were determined by Hitchens and Bryant (*13*).

RESULTS

If the formalism of transition-state theory is adopted, the pressure dependence of the rate constant (k) yields the activation volume ($\Delta V^{\ddagger}$) for the hydrogen exchange reaction at each amide site. Although reservations exist about employing transition-state theory as an analytical tool (*25*, *26*), it is, at least, a useful method for parametrizing the data and discussing the results. The concern is that the pressure dependence of the kinetic barrier may result from sources that cannot be properly accounted for using transition-state formalism. However, the measured exchange rates in the folded protein are slow compared to the intrinsically rapid chemical exchange rate of amide protons with solvent protons or deuterons, suggesting that relatively slow unfolding or penetration events dominate the observed exchange rates. Thus, the system appears to satisfy the requirements of a model built on statistical fluctuations such as transition-state theory, which we adopt to analyze these data.

The activation parameters can be extended to include a $P\Delta V^{\ddagger}$ term as shown in eq 5:

$$k = \frac{k_b T}{h} \exp(-\Delta H^{\ddagger}/RT) \exp(\Delta S^{\ddagger}/R) \exp(-P\Delta V^{\ddagger}/RT) \quad (5)$$

As discussed previously (*13*), the observed activation volume may have several contributions and can be expressed as the sum of three terms:

$$\Delta V^{\ddagger}_{obs} = \Delta V_s + \Delta V^{\ddagger}_{k_{OH}} + \Delta V_{K_W} \quad (6)$$

$\Delta V^{\ddagger}_{k_{OH}}$ is the activation volume of the base-catalyzed chemical exchange process, ΔV_{K_W} is the volume change associated with the ionization of water, and ΔV_s is the volume change associated with the accessibility of solvent to the amide site. Values for ΔV_{K_W} (−20.9 cm^3 mol^{-1}) and $\Delta V^{\ddagger}_{k_{OH}}$ (10.9 cm^3 mol^{-1}) have been reported previously (*27*−*30*). Substitution of these two values into eq 6 and rearrangement yield a volume associated with the energy barrier to the exchange event that we have called an accessibility volume. The solvent accessibility volumes for 42 amide sites in T4 lysozyme at 22 °C are summarized in Table 1 for comparison with activation enthalpies and entropies measured here (*13*).

The activation enthalpies ($\Delta H^{\ddagger}_{EX}$) and entropies ($\Delta S^{\ddagger}_{EX}$) for 42 amide sites in T4 lysozyme are summarized graphically in Figures 1 and 2. The range of temperatures (7−32 °C) was selected to encompass the temperature at which the activation volumes were measured (22 °C) and to avoid approach to unfolding transitions. The corrected activation enthalpies ($\Delta H^{\ddagger}_{EX}$) range from 7.3 to 34.0 kcal mol^{-1}. The corrected activation entropies ($\Delta S^{\ddagger}_{EX}$) range from −18.4 to 66.6 cal mol^{-1} K^{-1}.

A plot of the activation enthalpies versus the entropies is linear as shown in Figure 3 with a slope of 304 K and an intercept of 13.5 kcal mol^{-1}. A plot of the activation enthalpies versus the activation volumes results in a scatter plot with no apparent correlation between the variables as shown in Figure 4. A similar result obtained for the activation entropies compared with the activation volumes is not shown.

Protection factors were calculated for the 42 residues of the C54T/C97A mutant that were studied and are summarized in Table 1. These protection factors were calculated according to the method of Bai and co-workers (*23*) which includes the effects of neighboring residues on the reference exchange rate constant for the random coil form, k_{rc}. The log of the protection factors computed this way for the mutant ranges from 2.9 to 4.9. The protection factors reported for wild-type T4 lysozyme calculated previously by Dahlquist and co-workers are also summarized in Table 1 (*24*). The protection factor values for the mutant cannot be easily compared with those for the wild-type because the wild-type results reported by the Dahlquist group represent an average over a range of pH values.

DISCUSSION

The activation enthalpies ($\Delta H^{\ddagger}_{EX}$) for amide hydrogen exchange for the 42 residues measured range from 7.3 to

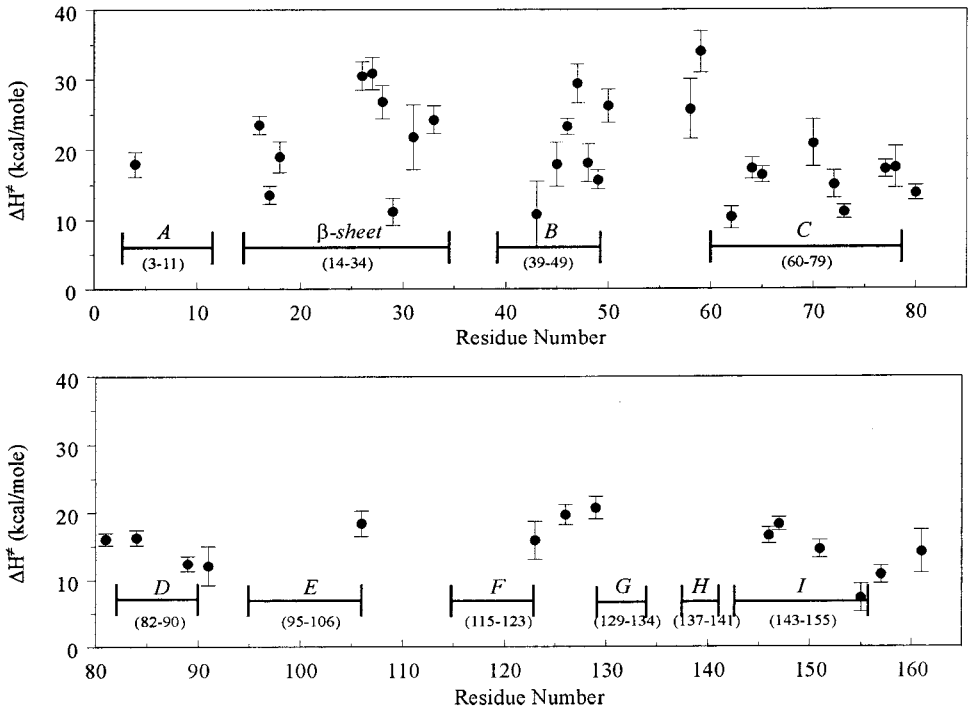

FIGURE 1: Activation enthalpies for hydrogen−deuterium exchange of WT* T4 lysozyme determined by the effect of temperature (280−305 K) on amide hydrogen exchange kinetics plotted as a function of residue number. Measured activation enthalpies were determined with eq 1 using kinetic data acquired at six temperatures. Error bars represent a 67% confidence interval of the fit. The bars in the plots indicate secondary structural elements of the protein. Letters represent each of the nine helices.

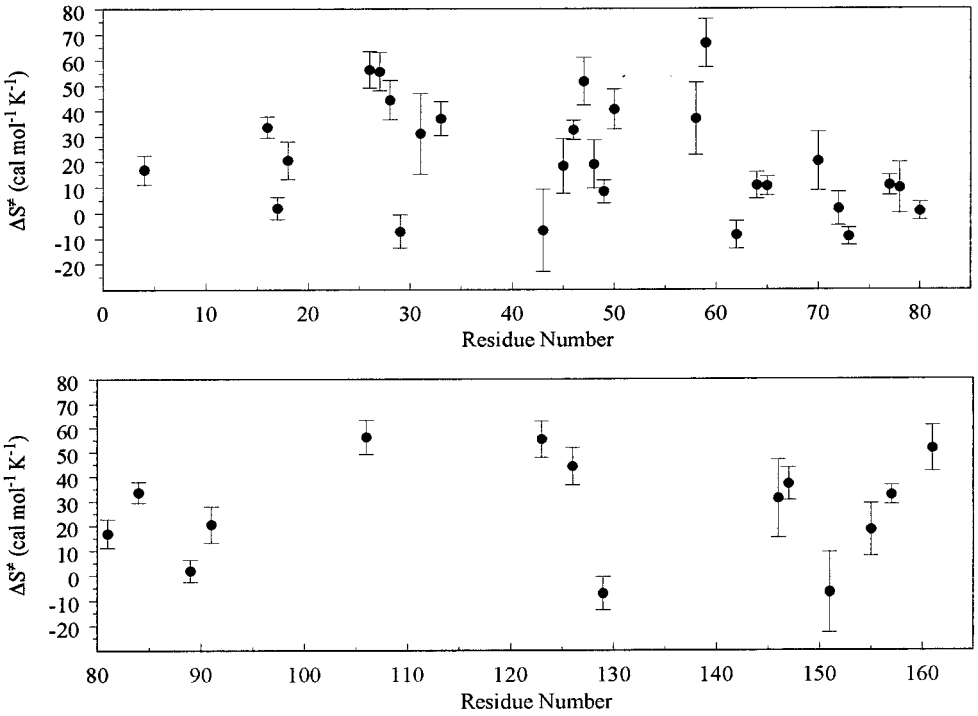

FIGURE 2: Activation entropies for hydrogen−deuterium exchange of WT* T4 lysozyme plotted as a function of residue number. Error bars represent a 67% confidence interval of the fit.

34.0 kcal mol^{-1}, which is a range well beyond the average experimental errors that are on the order of ±2 kcal mol^{-1}. These values are in the range usually reported for amide exchange from folded proteins (*31*, *32*). Figure 1 demonstrates that the enthalpic contribution to the activation barrier may be significantly different for residues that may be close in the amino acid sequence. Examples include Lys16 and Ile17, Gly28 and Ile29, Asp47 and Lys48, and Ala49 and Ile50. In other cases, the values are similar, for example, Thr26 and Ile27 in the β-sheet, Glu64 and Lys65, and Gly77 and Ile78 in the C-helix. The B-helix, the C-helix, and the β-sheet provide sufficient data for interesting comparisons. In the B-helix, $\Delta H^{\ddagger}_{EX}$ increases for each residue approaching Asp47 from either side. Asp47 has one of the largest

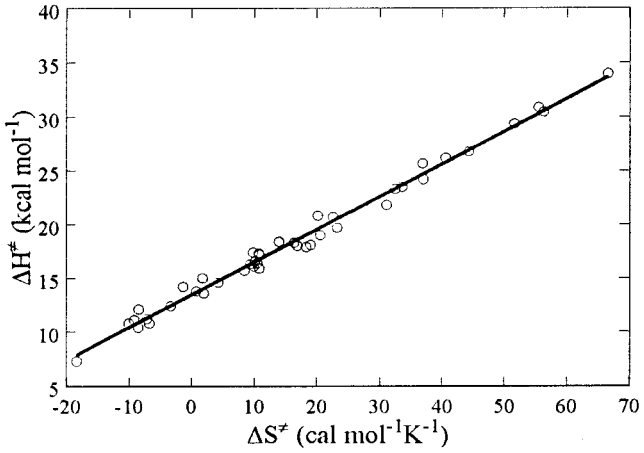

FIGURE 3: Activation enthalpy vs activation entropy for 42 amide sites in T4 lysozyme. The least-squares line indicated has a slope of 303.6 K and an intercept of 13.5 kcal mol^{-1}.

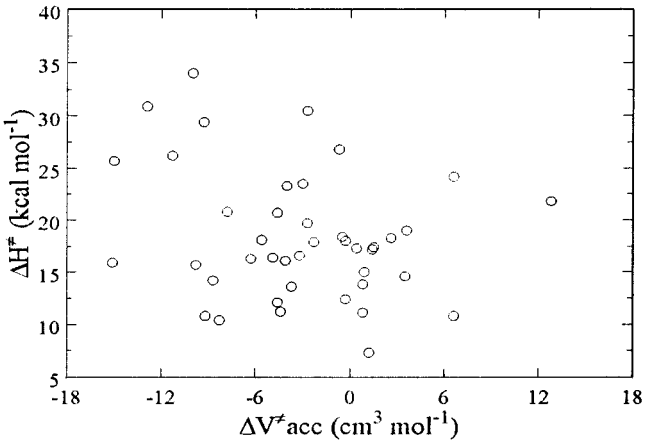

FIGURE 4: Activation enthalpy vs activation volume for 42 amide sites in T4 lysozyme.

activation enthalpies in this data set, 29.4 kcal mol^{-1}. The long C-helix connecting the C- and N-terminal domains has a number of slowly exchanging amide sites that are not characterized in this study. For those sites measured, however, the range of values is relatively narrow and all $\Delta H^{\ddagger}_{EX}$ are smaller than 20.8 kcal mol^{-1}. It is interesting that the largest activation enthalpy measured for the C-helix is again located in the middle of the helix.

Not all the residues in the β-sheet region fall in the sampling window of the experiments reported here. The loop regions exchange rapidly and are not reported. Figure 5 summarizes results for the β-sheet region schematically. The residues measured in the β-sheet that are hydrogen bonded to the central strand (Lys16 and Tyr18) have large activation enthalpies. Ile17, which hydrogen bonds in the other direction, has a small activation enthalpy. Thr26, Ile27, and Gly28, all on the central strand, have large activation enthalpies, but Ile29, which is in the beginning of the loop region, has an activation enthalpy that is only 11.2 kcal mol^{-1}. His31 and Leu33 located in the C-terminal strand of the β-sheet structure have similar activation enthalpies of 21.8 and 24.2 kcal mol^{-1}, respectively even though His31 participates in a salt bridge with Asp70. Leu32, on the other hand, exchanges too rapidly to fall in the observation window of these experiments.

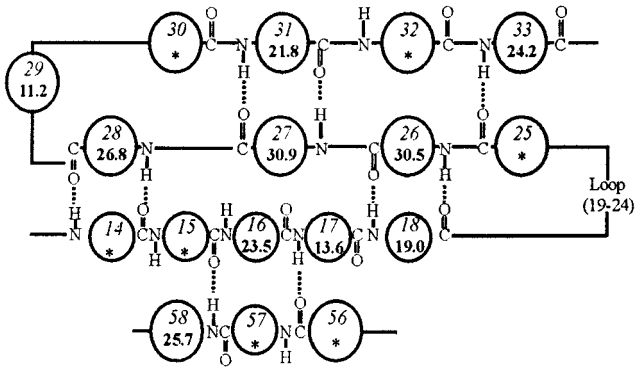

FIGURE 5: Schematic of the β-sheet region of T4 lysozyme with hydrogen bonds shown in dashed lines. Residue numbers are displayed in italic font, and $\Delta H^{\ddagger}_{EX}$ values for measured residues are indicated in bold font. An asterisk (*) indicates that exchange occurred too rapidly to be measured under the experimental conditions utilized.

For the class of mechanistic models that may be written

$$\text{rate} = K_{eq} k_{OH} [OH^-] \tag{7}$$

the activation parameters may be written as the sum of contributions:

$$\Delta G^{\ddagger}_{obs} = \Delta G^{\ddagger}_{k_{OH}} + \Delta G_{K_{eq}} + \Delta G^{\ddagger}_{K_W} - \Delta G_{Tris} \tag{8}$$

where the last two terms derive from the temperature dependence of the K_W and acid dissociation constant of the buffer, and the first two derive from the coefficients of [OH$^-$] in eq 7. $\Delta G^{\ddagger}_{k_{OH}}$ represents the contribution from the chemical step and $\Delta G_{K_{eq}}$ the contribution from the accessibility or equilibrium steps that bring the system to the reactive condition.

In the case where $\Delta G^{\ddagger}_{k_{OH}}$ may be measured in reference compounds, it varies over a narrow range of order ± 1 kcal mol^{-1}. This variation was included in computing protection factors in Table 1. However, because of possible $\Delta H^{\ddagger} - \Delta S^{\ddagger}$ compensation and possibly the large changes in both relative to $\Delta G^{\ddagger}$, it is somewhat speculative to presume that all changes in $\Delta G^{\ddagger}_{k_{OH}}$ result from neighbor effects on $\Delta H^{\ddagger}$. While it is reasonable to assume that variations in $\Delta H^{\ddagger}_{k_{OH}}$ are small compared to variations in $\Delta H^{\ddagger}_{obs}$, there appears to be little advantage in assuming that all $\Delta H^{\ddagger}_{k_{OH}}$ are identical to that for a reference compound such as poly-DL-alanine (*33*). Thus, in the context of the class of models represented by eq 7, we tabulate activation parameters corrected for the temperature dependence of K_W and K_{Tris} but leave the remainder as a sum of contributions associated with K_{eq} and k_{OH}. We denote these sums with a subscript EX for convenience. Nevertheless, the variations in $\Delta H^{\ddagger}_{EX}$ and $\Delta S^{\ddagger}_{EX}$ are large. The values of $\Delta H^{\ddagger}_{EX}$ range from 7.3 to 34.0 kcal mol^{-1}.

Even though the possibility of $\Delta H^{\ddagger} - \Delta S^{\ddagger}$ compensation makes neighbor effects for reference compounds difficult to estimate, this range of $\Delta H^{\ddagger}_{EX}$ appears to be too large to be dominated by neighbor effects. Thus, a reasonable hypothesis is that these variations are dominated by the accessibility factors for the coincidence of the reactants summarized by the factor K_{eq}. This hypothesis is supported by the observation that the activation enthalpies for reference compounds are

reported to be approximately 17 kcal mol^{-1} (*33*, *34*). When corrected for the temperature dependence of the water ionization constant, the reference enthalpy is on the order of 3.5 kcal mol^{-1} (*34*), which is much smaller than the values reported for any of the amide sites measured in the present study.

The activation entropies ($\Delta S^{\ddagger}_{EX}$) range from −18.4 to 66.6 cal mol^{-1} K^{-1} for the residues in the observation window. Figure 3 demonstrates that within experimental error, there is a linear relationship between $\Delta H^{\ddagger}$ and $\Delta S^{\ddagger}$. Entropy−enthalpy compensation is not uncommon (*35*). There has been concern that sampling errors and covariance may contribute to apparent correlation that is not fundamental (*36*, *37*). In the present case, it is crucial to note that the range of rate constants sampled is relatively narrow, about a factor of 100. With this range of rate constants, the range of the free energy of activation is small, spanning values from 20.7 to 23 kcal mol^{-1}. The consequence of this narrow range in $\Delta G^{\ddagger}$ is that if $\Delta H^{\ddagger}$ varies significantly then $\Delta S^{\ddagger}$ must vary correspondingly to maintain $\Delta G^{\ddagger}$ within this window. If this were not true, then the rate constant would quickly fall outside the observation window. Thus, the linear relationship between $\Delta H^{\ddagger}$ and $\Delta S^{\ddagger}$ is at least partly a consequence of the narrow sampling window constraint on $\Delta G^{\ddagger}$.

The experimental errors in the values of $\Delta H^{\ddagger}$ and $\Delta S^{\ddagger}$ are too large to permit a meaningful assessment of $\Delta H^{\ddagger}-\Delta S^{\ddagger}$ compensation beyond that required by the constraints provided by the sampling window. Nevertheless, the changes in $\Delta H^{\ddagger}$ are well outside experimental error; the range of values is nearly 10 times the experimental error. Thus, even though the range of $\Delta G^{\ddagger}$ is small, there are large variations in both $\Delta H^{\ddagger}$ and $\Delta S^{\ddagger}$, which reflect differences in the energetic requirements of the hydrogen exchange pathway. In this context, the rather large differences in activation parameters, which may be observed for residues that are close together in the sequence, suggest that pathways for hydrogen exchange at closely related sites might differ considerably in energetic detail.

An interesting feature of amide hydrogen exchange is that most often the rank order of the exchange is preserved as the temperature changes (*38*, *39*). This observation is one of the direct consequences of the linear relationship between $\Delta H^{\ddagger}$ and $\Delta S^{\ddagger}$, a point noted earlier by Gregory and Lumry (*35*).

Figure 4 shows that for the 42 amide sites studied, the activation volumes for amide proton exchange are not correlated with the activation enthalpies. Because the enthalpy is proportional to the entropy, the activation volume is not correlated with the activation entropy either. This result is reasonable because the magnitudes of $P\Delta V^{\ddagger}$ are small compared with $\Delta H^{\ddagger}$ or $T\Delta S^{\ddagger}$. Similarly, there is no significant correlation between $\Delta V^{\ddagger}$ and protection factors.

CONCLUSIONS

Measurements of activation parameters $\Delta H^{\ddagger}$, $\Delta S^{\ddagger}$, and $\Delta V^{\ddagger}$ for amide proton exchange at 42 sites in T4 lysozyme show that $\Delta S^{\ddagger}$ and $\Delta H^{\ddagger}$ are linearly correlated, in major part as a consequence of a narrow sampling window for $\Delta G^{\ddagger}$, i.e., a narrow range of rate constants. This entropy−enthalpy compensation accounts for the preservation of the rank order of exchange over the temperature range from 273 to 323 K. The values of $\Delta V^{\ddagger}$ do not correlate with either $\Delta H^{\ddagger}$ or $\Delta S^{\ddagger}$ for the sites studied which is consistent with the small contribution that the $P\Delta V^{\ddagger}$ term makes to $\Delta G^{\ddagger}$. Finally, the variations in $\Delta H^{\ddagger}$, $\Delta S^{\ddagger}$, and $\Delta V^{\ddagger}$ for residues that are structurally close together in the folded protein suggest different pathways for the access of solvent to these exchange sites.

ACKNOWLEDGMENT

We thank Professors Clare Woodward, Rodney Biltonen, Rufus Lumry, Wayne Bolen, Andrew Robertson, and Kazuyuki Akasaka for helpful discussions.

REFERENCES

1. Sternberg, M. J. E., Grace, D. E. P., and Phillips, D. C. (1979) *J. Mol. Biol. 130*, 231−253.
2. Artymiuk, P. J., Blake, C. C. F., Grace, D. E. P., Oatley, S. J., Phillips, D. C., and Sternberg, M. J. E. (1979) *Nature (London) 280*, 56.
3. Lakowicz, J. R., and Weber, G. (1973) *Biochemistry 12*, 4171−4179.
4. Munro, I. M., Pecht, I., and Stryer, L. (1979) *Proc. Natl. Acad. Sci. U.S.A. 12*, 56−60.
5. Wagner, G., and Wüthrich, K. (1986) *Methods Enzymol. 131*, 307−326.
6. Woodward, C. K., and Hilton, B. D. (1979) *Annu. Rev. Biophys. Bioeng. 8*, 99−127.
7. Woodward, C., Simon, I., and Tüchsen, E. (1982) *Mol. Cell. Biochem. 48*, 135−160.
8. Hvidt, A., and Nielsen, S. O. (1966) *Adv. Protein Chem. 21*, 287−386.
9. Englander, S. W., and Kallenbach, N. R. (1984) *Q. Rev. Biophys. 16*, 521−655.
10. Englander, S. W., Sosnick, T. R., Englander, J. J., and Mayne, L. (1996) *Curr. Opin. Struct. Biol. 6*, 18−23.
11. Miller, D. W., and Dill, K. A. (1995) *Protein Sci. 4*, 1860−1873.
12. Swint-Kruse, L., and Robertson, A. D. (1996) *Biochemistry 35*, 171−180.
13. Hitchens, T. K., and Bryant, R. G. (1998) *Biochemistry 37*, 5878−5887.
14. Muchmore, D. C., McIntosh, L. P., Russell, C. B., Anderson, D. E., and Dahlquist, F. W. (1989) *Methods Enzymol. 177*, 44−73.
15. Anderson, D. E., Becktel, W. J., and Dahlquist, F. W. (1990) *Biochemistry 29*, 2403−2408.
16. Matsumura, M., and Matthews, B. W. (1989) *Science 243*, 792−794.
17. Zhang, O., Kay, L. E., Olivier, J. P., and Forman-Kay, J. D. (1994) *J. Biomol. NMR 4*, 845−858.
18. Kay, L. E., Keifer, P., and Saarinern, T. (1992) *J. Am. Chem. Soc. 114*, 10663−10665.
19. Johnson, M. L. (1994) *Methods Enzymol. 240*, 1−22.
20. Johnson, M. L., and Frasier, S. G. (1985) *Methods Enzymol. 117*, 301−342.
21. Harned, H. S., and Owen, B. B. (1950) *ACS Monograph 95*, p 514, Reinhold Publishers, New York.
22. Bates, R. G., and Hetzer, H. B. (1961) *J. Phys. Chem. 65*, 667.
23. Bai, Y., Milne, J. S., Mayne, L., and Englander, S. W. (1993) *Proteins 17*, 75−86.
24. Anderson, D. E., Lu, J., McIntosh, L., and Dahlquist, F. W. (1993) in *NMR of Proteins* (Clore, G. M., and Gronenborn, A. M., Eds.) pp 258−304, CRC Press, Ann Arbor, MI.
25. Skinner, J. L., and Wolynes, P. G. (1978) *J. Phys. Chem. 69*, 2143−2150.
26. Karplus, M., and McCammom, J. A. (1981) *CRC Crit. Rev. Biochem. 9*, 235−293.
27. Carter, J. V., Knox, D. G., and Rosenberg, A. (1978) *J. Biol. Chem. 253*, 1947−1953.

28. Isaacs, N. S. (1981) *Liquid-Phase High-Pressure Chemistry*, John Wiley and Sons, New York.
29. Morild, E. (1981) *Adv. Protein Chem. 34*, 93−166.
30. VanEldick, R., Asano, T., and LeNobel, W. J. (1989) *Chem. Rev. 89*, 549−688.
31. Woodward, C. K., and Hilton, B. D. (1980) *Biophys. J. 32*, 561−575.
32. Thomsen, N. K., and Poulsen, F. M. (1993) *J. Mol. Biol. 234*, 234−241.
33. Englander, S. W., and Poulsen, A. (1969) *Biopolymers 7*, 379−393.
34. Englander, S. W., Downer, N. W., and Teitelbaum, H. (1972) *Annu. Rev. Biochem. 41*, 903−924.
35. Gregory, R. B., and Lumry, R. (1985) *Biopolymers 24*, 301−326.
36. Krug, R. R., Hunter, W. G., and Grieger, R. A. (1976) *J. Phys. Chem. 80*, 2335−2341.
37. Krug, R. R., Hunter, W. G., and Grieger, R. A. (1976) *J. Phys. Chem. 80*, 2341−2351.
38. Woodward, C. K., and Rosenberg, A. (1971) *J. Biol. Chem. 246*, 4105−4113.
39. Gregory, R. B., Dinh, A., and Rosenberg, A. (1986) *J. Biol. Chem. 261*, 13963−13968.

BI991718Y